Effect of Ionic Liquids as Additives on Lithium Electrolytes: Conductivity, Electrochemical Stability, and Aluminum Corrosion†

Dominik Moosbauer, Sandra Zugmann, Marius Amereller, and Heiner J. Gores*

Institute of Physical and Theoretical Chemistry, University of Regensburg, Universitätsstrasse 31, D-93040 Regensburg, Germany

We investigated the influence that eight ionic liquids (ILs) as additives have on the conductivity and electrochemical stability of lithium salt-based electrolytes. The investigated salts were the well-known lithium hexafluorophosphate ($LiPF_6$), which is the preferred salt for lithium ion batteries (LIBs), and the new salt lithium difluoro(oxalato)borate (LiDFOB). Conductivity studies performed over the temperature range (238.15 to 333.15) K showed a temperature-dependent increase in conductivity caused by several IL additives. The electrochemical stabilities of the solutions were determined at platinum and aluminum electrodes. At the Pt electrode, $LiPF_6$ is the more stable salt, whereas at the aluminum electrode, LiDFOB exhibits a 0.5 V higher potential window in comparison with $LiPF_6$-based solutions. An investigation of the influence of added ILs on the corrosion of aluminum, the current collector material for cathodes of LIBs, did not reveal any adverse effects.

Introduction

The performance of lithium ion batteries (LIBs) is affected by many parameters of the electrolyte, including voltage window, conductivity, diffusion, and lithium ion transference number. In the battery, the electrolyte determines the corrosion behavior of the cathodic aluminum current collector. To the aluminum surface is attached an active cathode material, such as a layered metal oxide (Li_xMO_2, M = Co, Ni, Mn), spinel-structured $Li_xMn_2O_4$, or Li_xFePO_4.[1−5] Aluminum is still in contact with the electrolyte and may corrode via oxidative dissolution (pitting corrosion),[6−9] entailing the inactivation of the whole cathode. However, a passivation layer can be formed on the aluminum surface, protecting the Al from further corrosion.

The commonly used salt lithium hexafluorophosphate ($LiPF_6$) shows good properties in forming a stable passivation layer that prevents further Al corrosion.[9,10] This salt exhibits very good conductivity and electrochemical stability; therefore, it is preferred in LIBs. However, this salt shows some problems, including low thermal stability and the formation of the Lewis acid PF_5, which hydrolyzes to HF and POF_3 and may polymerize solvents.[11,12] These problems have pushed a continuing search for better lithium salts.[13−17] Synthesized lithium bis(trifluoromethylsulfonyl)imide [LiTFSI, $Li(CF_3SO_2)_2N$] shows good thermal stability and relatively high conductivity but is poor in Al protection.[18] Lithium bis[oxalato(2−)]borate [LiBOB, $LiB(C_2O_4)_2$] was reported to have a very good protecting property and thermal stability,[17,19,20] but it suffers from low solubility in carbonate solvents and low conductivity.[21,22]

Lithium difluoro(oxalato)borate (LiDFOB, $LiBF_2C_2O_4$) combines some positive aspects of LiBOB and $LiPF_6$ and shows improved performance at low temperatures. LiDFOB is much more soluble than LiBOB in many organic solvents and blends, forms a stable solid electrolyte interface (SEI), and provides a wide operational temperature range.[23] Recently, we successfully synthesized this salt without chloride impurities via a new synthetic approach.[24] Besides the search for new lithium salts for better performance, compatible additives can be added to the electrolyte. These additives can improve the properties of the electrolyte, its conductivity,[25,26] and its electrochemical stability by forming passivation layers on the electrodes,[27] preventing corrosion of the Al current collector of the cathode.

In the present work, we studied the potential of ionic liquids (ILs) that have melting points below 373.15 K as electrolyte additives for improving the performance of the electrolytes. These ILs contain unsymmetrical cations or anions in a sterically demanding form, entailing charge delocalization and subsequent weak association.

Since ILs exhibit very low vapor pressure and are nonflammable, they also may be a good alternative as the solvent for LIB electrolytes, which usually are organic carbonates.[28,29] Unwelcome disadvantages of ILs mainly are the high production cost and a rather high viscosity, in comparison with the organic solvents. By the right choice of the components (i.e., the cations and anions), the viscosities of ILs can be significantly reduced. Such ILs are believed to be suitable as additives for electrolytes to improve the performance of LIBs.

Experimental Section

Lithium Salts. Two different salts, $LiPF_6$ (Stella, high purity) and LiDFOB, were investigated. LiDFOB was synthesized using our previously described route.[24] NMR analysis showed no impurities [see Figures S1−S4 in the Supporting Information (SI)], and the water mass fraction was low ($< 5 \cdot 10^{-5}$), as checked by Karl Fischer titration (Mettler Karl Fischer Titrator DL18). This salt was expected to combine the merits of $LiPF_6$ and LiBOB, namely, wide electrochemical and thermal stability, high conductivity, good solubility, and ability to form a passivation layer on aluminum.

Conductivity Measurements. In order to reach a high conductivity at low temperatures, a mixture of ethylene carbonate (1) + dimethyl carbonate (2) + ethyl methyl carbonate (3) (EC + DMC + EMC, with mass fractions $w_1 = 0.1$, $w_2 = 0.25$,

† Part of the "Josef M. G. Barthel Festschrift".

* Corresponding author. Phone: + 49 (0)941 943 4746. Fax: + 49 (0)941 943 4532. E-mail: heiner.gores@chemie.uni-regensburg.de.

10.1021/je900867m © 2010 American Chemical Society
Published on Web 02/01/2010

and $w_3 = 0.65$) was used as the solvent. A series of electrolytes with salt concentrations ranging from (0.2 to 2.0) mol·L^{-1} was prepared. The exact salt concentrations were calculated by determining the densities of the solutions at the respective temperatures with a precision densitometer (Anton Paar DMA 60/DMA 602). For studies of IL additives, the selected ILs were added (mass fraction $w = 0.1$) to a 1.45 mol·L^{-1} lithium salt electrolyte. Table S5 in the SI shows the acronyms, chemical structures, and names of the cations and anions in the ILs used in this work.

The conductivity was measured using our capillary cells[30] that were filled with the electrolyte in a glovebox and closed air-tight. Before the measurements, the cells were calibrated with a 0.1 mol·L^{-1} solution of KCl in triply distilled water. The cells were thermostatted (with a temperature stability of ± 1 mK) by controlling the temperature with a setup including a cryostat (Holzwarth HM 90 EW), power supply (EA-PS 3065-10 B), PID controller, sinus generator, and resistance decade.[31,32] The resistances were recorded at (1.7, 3.2, 5.1, 6.5, 7.7, and 10.1) kHz. Plotting of the measured resistances against reciprocal frequency followed by an extrapolation to infinite frequency enabled the definition of the electrolyte resistance. Therefore, we were able to evaluate conductivities with an accuracy of 0.01%.

Cyclic Voltammetry Experiments. The cyclic voltammetry measurements were carried out in a 1 M solution of the lithium salt in the standard blend of ethylene carbonate (1) + diethyl carbonate (2) (EC + DEC, $w_1 = 0.3$, $w_2 = 0.7$). All of the solvents were purchased from Merck KGaA Darmstadt (p.a.) and showed a water mass fraction of less than $1 \cdot 10^{-5}$ (Mettler Karl Fischer Titrator DL18). The electrolyte solutions were all prepared in a glovebox (Mecaplex GB80) with low mass fractions of water ($< 1 \cdot 10^{-6}$) and oxygen ($< 5 \cdot 10^{-6}$). Addition of various ILs (Table S5 in the SI) with a mass fraction of $w = 0.1$ enabled the investigation of the influence of the ILs on the electrochemical stability.

The electrochemical stability was measured on two working electrodes: an Al foil (area = 0.787 cm^2) and a Pt electrode with a surface area of 0.0707 cm^2. The Al foil was rinsed with acetone (p.a.) and the Pt working electrode polished using a polycrystalline diamond spray before every measurement. A Pt sheet served as the counter electrode. Comparing measurements with a Li counter electrode showed no changes. As the reference electrode for the measurements on Pt, an Ag/Ag$^+$ cryptand electrode was used. This Izutsu-type electrode consisted of a solution of 0.1 mol·L^{-1} $AgNO_3$ (Carl Roth GmbH+Co., p.a.) and 0.2 mol·L^{-1} Kryptofix 22 (Merck, for synthesis) in acetonitrile with a silver wire as the current collector and glassy ceramic Vycor (BAS) as the conductive membrane to separate the reference electrode and the electrolyte. The potential of the reference electrode was controlled by adding a small amount of ferrocene, so the potentials could be exactly converted to the Li/Li$^+$ scale. A Li pseudoreference electrode was used for the measurements with Al foil as the working electrode. All of the cyclic voltammetry experiments were performed on a Reference 600 potentiostat/galvanostat (Gamry Instruments) at potential sweep rates (υ) of (20 and 5) mV·s^{-1} respectively.

Results and Discussion

Conductivity. Figure S6 in the SI shows the dependence of the specific conductivity (κ) of $LiPF_6$ electrolytes on temperature and salt concentration. The maximal conductivity κ_{max} is 8.97 mS·cm^{-1}, which was reached at the corresponding molality μ of 1.50 mol·kg^{-1} (equal to 1.41 mol·L^{-1}) at 303.15 K, as determined by fitting the data to the Casteel−Amis equation (eq 1):[33]

$$\kappa = \kappa_{max}\left(\frac{m}{\mu}\right)^a \exp\left[b(m-\mu)^2 - \frac{a}{\mu}(m-\mu)\right] \qquad (1)$$

where m is the molality of the electrolyte and a and b are fit parameters.

The measured specific conductivities are in good agreement with those for $LiPF_6$ solutions in the literature. In EC (1) + DMC (2) ($w_1 = 0.5$, $w_2 = 0.5$), a 1 M solution at 298.15 K shows a conductivity of 10.7 mS·cm^{-1},[34] and in PC (1) + DEC (2) ($w_1 = 0.4$, $w_2 = 0.6$), a 1 mol·kg^{-1} solution at 303.15 K has a conductivity of 5.0 mS·cm^{-1}.[35]

In comparison with the results for LiDFOB-based electrolytes (see Figure 1), the conductivities of $LiPF_6$ electrolytes are much higher. The maximal conductivity for LiDFOB over the temperature range we measured is about 5.24 mS·cm^{-1}, which was reached at 1.65 mol·kg^{-1} (equal to 1.54 mol·L^{-1}) at 303.15 K; this value is a little more than the half of the highest conductivity of the $LiPF_6$-based electrolytes. In both cases, the concentrations corresponding to the highest conductivity decrease with decreasing temperature (see Tables S7 and S8 in the SI) because of an increase in the viscosity at lower temperatures.

Addition of Ionic Liquids. Figure 2 shows the specific conductivity of $LiPF_6$ electrolytes with added ILs ($w = 0.1$). The specific conductivities at 298.15 K are in the range (6.35 to 8.25) mS·cm^{-1}. The addition of two ILs (bmpl ntf and bmpl fap) raises the conductivity of the electrolyte, mainly at high temperatures above 323.15 K, to a minor degree. Below 313.15 K, the additive effect no longer exists, which can be attributed to the greatly increased viscosity of the ILs at low temperatures. With respect to the cations of the ILs, the cyclic-structured pyrrolidinium and imidazolium cations show the best results because of the effect of the sizes of these cations relative to the linear-structured and very large P(h3)t cation. The cyclic-structured cations are smaller, which results in lower viscosity. The measurements show further that the ntf and fap anions add more to the conductivities than the linear P(h3)t cations, while the smaller otf anion depresses the conductivity tentatively, as explained by its higher degree of association with Li$^+$ ions.

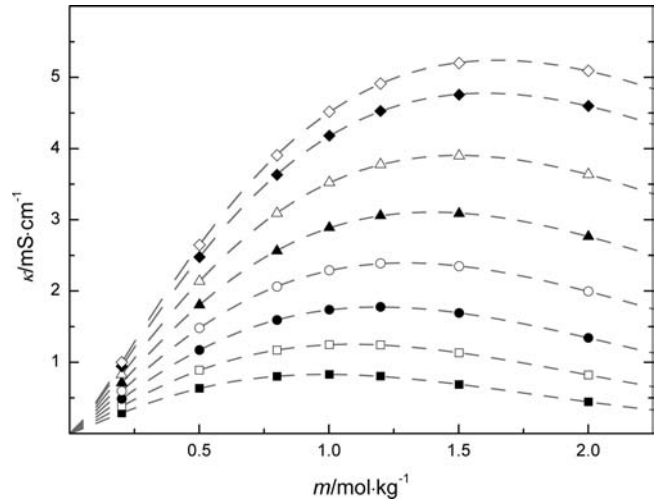

Figure 1. Dependence of the specific conductivity κ of LiDFOB on the molal concentration m in EC (1) + DMC (2) + EMC (3) ($w_1 = 0.1$, $w_2 = 0.25$, $w_3 = 0.65$) at different temperatures: ◇, 303.15 K; ◆, 298.15 K; △, 288.15 K; ▲, 278.15 K; ○, 268.15 K; ●, 258.15 K; □, 248.15 K; ■, 238.15 K.

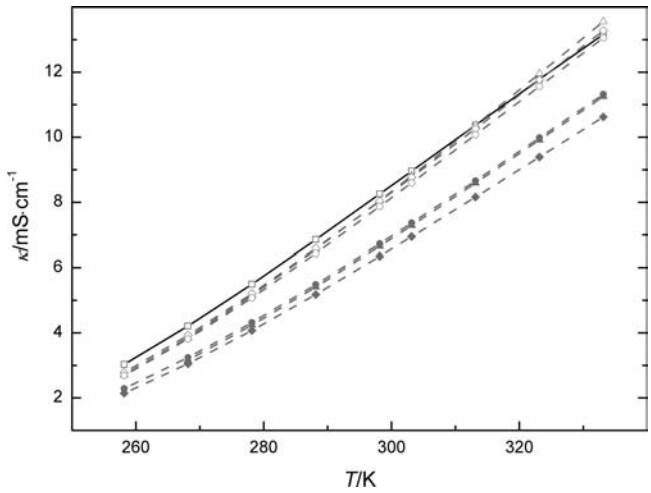

Figure 2. Temperature dependence of the specific conductivity κ of 1.45 M $LiPF_6$ in EC (1) + DMC (2) + EMC (3) ($w_1 = 0.1$, $w_2 = 0.25$, $w_3 = 0.65$) with IL additives ($w = 0.1$): □, without IL; △, bmpl fap; ◇, bmpl ntf; ●, bmpl otf; ○, hmim ntf; ▲, P(h3)t fap; ◆, P(h3)t ntf.

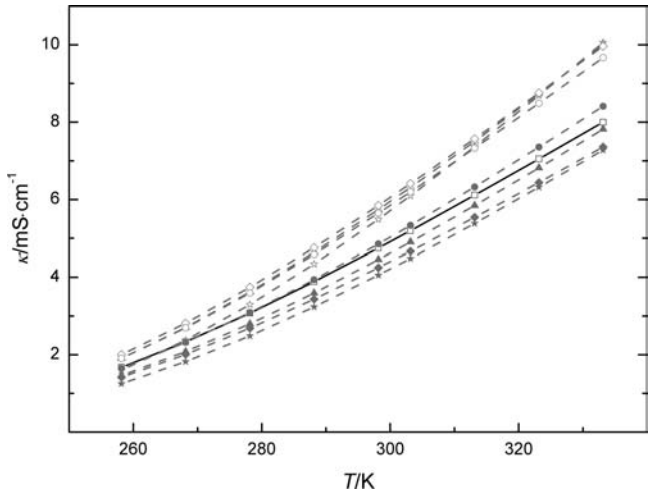

Figure 3. Temperature dependence of the specific conductivity κ of 1.45 M LiDFOB in EC (1) + DMC (2) + EMC (3) ($w_1 = 0.1$, $w_2 = 0.25$, $w_3 = 0.65$) with IL additives ($w = 0.1$): □, without IL; ☆, bmpl bob; △, bmpl fap; ◇, bmpl ntf; ●, bmpl otf; ○, hmim ntf; ★, P(h3)t bob; ▲, P(h3)t fap; ◆, P(h3)t ntf.

Similar trends were obtained for LiDFOB electrolytes (see Figure 3), but here the additive effect is significantly higher. Whereas the pure LiDFOB electrolyte has a lower specific conductivity at 298.15 K (4.75 $mS \cdot cm^{-1}$) than the $LiPF_6$ electrolyte (8.25 $mS \cdot cm^{-1}$), the improvement due to additives is much more significant. The enhancement in the conductivity at higher temperatures is up to 25% and much larger than those observed with $LiPF_6$ electrolytes. Mainly hmim ntf, bmpl ntf, and bmpl fap as well as bmpl bob show very good results. Here the increase in the conductivity at high temperatures is much more pronounced than at lower temperatures, showing the stronger temperature dependence of the viscosity because of a higher melting point. The IL bmpl bob is the only investigated salt that is not a room-temperature ionic liquid (RTIL), but this does not affect the conductivity improvement, especially at higher temperatures. Again, the ILs with P(h3)t cations or otf anions show less or no improvement.

Electrochemical Stability. Pt Working Electrode. Figure S9 in the SI shows the cyclic voltammogram of the $LiPF_6$ electrolyte at a Pt electrode. At 5.57 V vs Li/Li^+, the electrolyte starts to decompose (E_{ox}), as indicated by the anodic current, which increases dramatically to a preset value of 2 $mA \cdot cm^{-1}$. Near 0.27 V are small reductive currents, which correspond to the formation of Li−Pt alloy. Mass deposition of lithium metal occurs at −0.72 V. The potential difference between oxidative decomposition of the electrolyte and mass deposition of lithium leads to an electrochemical window of 5.30 V. This value is comparable to literature data.[36,37]

The oxidative decomposition of LiDFOB electrolyte occurs at 5.03 V, resulting in a value of 4.59 V for the electrochemical window. Table S10 in the SI displays the values of the potential windows for these IL-added electrolytes, which show that the addition of ILs does not significantly reduce the electrochemical window of $LiPF_6$ and LiDFOB electrolytes. Surprisingly, addition of fap ILs increases the oxidation potential of $LiPF_6$ electrolytes up to 6 V.

Al Working Electrode. The cell for measurements on Al was assembled in the glovebox, and measurements were performed in the anodic (positive) direction from 2 V to 8 V at a potential sweep rate of 5 $mV \cdot s^{-1}$ and then back to −0.5 V. In the first cycle for a 1 M solution of $LiPF_6$ (see Figure S11a in the SI), a sharp increase in the oxidative current occurs at about 3.55 V. At higher potentials, the current reaches a maximum and remains constant until the end of the anodic potential sweep, which can be attributed to the passivation of the aluminum surface. The consecutive cycles show increasing currents that do not decrease until higher potentials due to newly beginning passivation, indicating further decomposition of the electrolyte and dissolution of the aluminum.

The same measurements were carried out on a 1 M solution of LiDFOB (see Figure S11b in the SI). The first cycle shows behavior similar to that observed for the $LiPF_6$-based electrolyte. In this case, the sharp current increase occurs at 4.09 V, about 0.5 V higher than that observed for the $LiPF_6$ electrolyte. Because of the formation of the passivation layer, consecutive cycles result in lower currents that remain up to 7 V, which indicates a stronger passivation layer for LiDFOB than for $LiPF_6$.

Corrosion Behavior. For the study of Al corrosion, a current density of 0.25 $\mu A \cdot cm^{-2}$ was set to define the corrosion potential. Since aluminum foil is used only as a current collector for the cathode in LIBs, the studied potential range in this work was narrowed to the region from (2 to 5.5) V.

As shown in Figure 4, the anodic current of the first cycle of Al foil in 1 M $LiPF_6$ remains very low up to 3.50 V. From that point on, the current starts to increase dramatically and forms a peak at 3.94 V. After the peak, the current remains stable at a level of (5 to 6) $\mu A \cdot cm^{-2}$. These phenomena are attributed to anodic dissolution and resulting passivation of Al.[38,39] In the following scans, the current is decreased while the corrosion potential moves to higher values with scan number. In the electrochemically induced oxidation of Al, the resulting Al^{3+} ions are combined with the decomposition products of the electrolyte to form a protective passivation layer on the surface of Al.[10,18] It is known that LiTFSI has very poor corrosion-resistive properties.[40] The cyclic voltammogram in Figure 4 shows that the ILs with this anion (ntf) have no influence on the corrosion of Al. In these cases, the passivation layer already formed by $LiPF_6$ is stable. Only small changes in the corrosion potential and the current density are observable.

Cyclic voltammetry results for LiDFOB-based electrolytes show no major difference in the effect of ILs on Al corrosion (see Figure 5). Compared with $LiPF_6$-based electrolytes, LiDFOB electrolytes show later Al corrosion, as indicated by a 0.45 V higher decomposition potential and lower

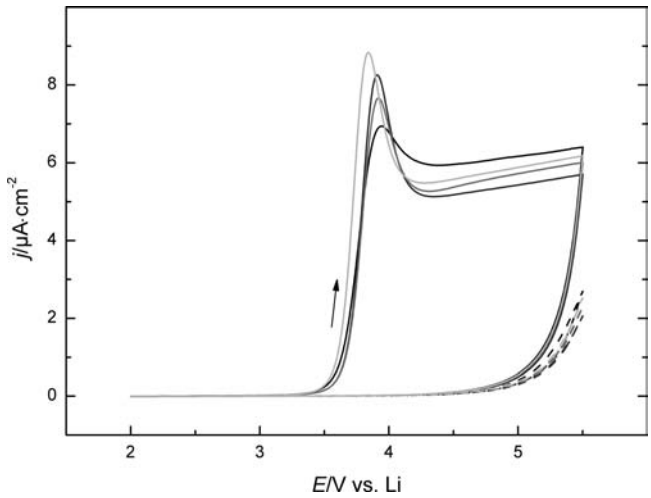

Figure 4. Cyclic voltammograms ($v = 5$ mV·s^{-1}) of 1 M $LiPF_6$ in EC (1) + DEC (2) ($w_1 = 0.3$, $w_2 = 0.7$) containing IL additives ($w = 0.1$) at the Al electrode; solid line, first cycle; dashed line, second cycle; black, without IL; dark-gray, bmpl ntf; gray, hmim ntf; light-gray, P(h3)t ntf. The arrow shows the direction of the forward scan.

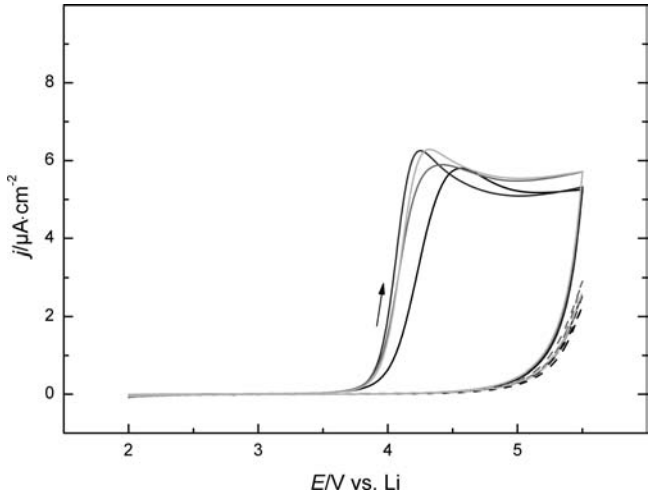

Figure 5. Cyclic voltammograms ($v = 5$ mV·s^{-1}) of 1 M LiDFOB in EC (1) + DEC (2) ($w_1 = 0.3$, $w_2 = 0.7$) containing IL additives ($w = 0.1$) at the Al electrode: solid line, first cycle; dashed line, second cycle; black, without IL; dark-gray, bmpl ntf; gray, hmim ntf; light-gray, P(h3)t ntf. The arrow shows the direction of the forward scan.

passivation current. The following scans yield 4.96 V for the decomposition potential, which is 0.1 V higher than that observed for $LiPF_6$. The results in Figure 5 show that the highly corrosive ntf anion has no adverse effect on Al corrosion and that the passivation layer already formed by DFOB anions is stable.

Conclusions

Conductivity measurements have shown that the addition of ILs can effectively increase the conductivity of $LiPF_6$- and LiDFOB-based electrolytes. This feature can be used to improve the power performance of LIBs. The best improvement in the ionic conductivity was obtained using ILs with low viscosity, including hmim ntf, bmpl ntf, and bmpl fap. In addition, bmpl bob is effective as an additive to increase conductivity. In LiDFOB-based electrolytes, the enhancement of the conductivity by additives was up to 25% and much higher than that observed in the $LiPF_6$-based electrolytes. Therefore, the conductivity gap between $LiPF_6$ and LiDFOB electrolytes can be reduced by use of IL additives.

Cyclic voltammetry measurements have shown that the electrochemical stability of $LiPF_6$ electrolytes on Pt is higher than that of LiDFOB. This trend is reversed in the case of the aluminum electrode, i.e., the passivation potential of Al by LiDFOB-based electrolytes is 0.45 V higher than for $LiPF_6$. Addition of ILs in electrolytes has no adverse effect on the passivation and stability of Al. Furthermore, addition of ntf ILs, in which the anion is highly corrosive to Al, has no influence on Al corrosion. The passivation layer formed by $LiPF_6$ and LiDFOB is still stable.

To check the possibility of ILs as solvent alternatives, pure ILs and their mixtures have to be used. These measurements give a first overview of the usefulness of several studied ILs.

Acknowledgment

The authors thank Prof. Dr. J. Barthel for introducing us to fundamental research in the field of the physical chemistry and electrochemistry of electrolyte solutions. The studies of our workgroup, Electrochemistry and Electrolytes, are based on his previous work and inspired by his continuous interest. The authors also thank Dr. Sheng Shui Zhang (U.S. Army Research Laboratory) for the discussion regarding the results of this study and for valuable suggestions.

Supporting Information Available:

NMR data for the synthesized LiDFOB (Figures S1−S4); chemical structures, names, and acronyms for the cations and anions of the ILs (Table S5); temperature and concentration dependence of the conductivity of $LiPF_6$ (Figure S6); Casteel−Amis parameters obtained from nonlinear fits of the specific conductivities of $LiPF_6$ (Table S7) and LiDFOB (Table S8); and cyclic voltammograms for $LiPF_6$ and LiDFOB on Pt and aluminum (Figures S9 and S11) and the corresponding decomposition potentials (vs Li/Li^+) of $LiPF_6$ and LiDFOB at Pt (Table S10). This material is available free of charge via the Internet at http://pubs.acs.org.

Literature Cited

(1) Yazami, R.; Lebrun, N.; Bonneau, M.; Molteni, M. High performance $LiCoO_2$ positive electrode material. *J. Power Sources* **1995**, *54*, 389–392.
(2) Thackeray, M. M. Manganese oxides for lithium batteries. *Prog. Solid State Chem.* **1997**, *25*, 1–71.
(3) Julien, C. 4-V cathode materials for rechargeable lithium batteries: wet-chemistry synthesis, structure and electrochemistry. *Ionics* **2000**, *6*, 30–46.
(4) *Materials for Lithium-Ion Batteries*; Julien, C., Stoynov, Z., Eds.; Kluwer: Dordrecht, The Netherlands, 2000.
(5) Whittingham, M. S. Lithium Batteries and Cathode Materials. *Chem. Rev.* **2004**, *104*, 4271–4301.
(6) Dalard, F.; Rais, A. B. Organic electrolytes for corrosion testing of aluminium and Al−Li binary alloys. *J. Appl. Electrochem.* **1989**, *19*, 157–161.
(7) Shembel, E. M.; Apostolova, R. D.; Strizhko, A. S.; Belosokhov, A. I.; Naumenko, A. F.; Rozhkov, V. V. Problems of corrosion and other electrochemical side processes in lithium chemical power sources with non-aqueous electrolytes. *J. Power Sources* **1995**, *54*, 421–424.
(8) Braithwaite, J.; Nagasubramanian, G.; Gonzales, A.; Lucero, S.; Cieslak, W. Corrosion of Current-Collector Material in Li-Ion Cells. In *Lithium Polymer Batteries*; Broadhead, J., Scrosati, B., Eds.; The Electrochemical Society: Pennington, NJ, 1997; pp 44−51.
(9) Zhang, S. S.; Jow, T. R. Aluminum corrosion in electrolyte of Li-ion battery. *J. Power Sources* **2002**, *109*, 458–464.
(10) Morita, M.; Shibata, T.; Yoshimoto, N.; Ishikawa, M. Anodic behavior of aluminum in organic solutions with different electrolytic salts for lithium ion batteries. *Electrochim. Acta* **2002**, *47*, 2787–2793.
(11) Andersson, A. M.; Edstrom, K. Chemical composition and morphology of the elevated temperature SEI on graphite. *J. Electrochem. Soc.* **2001**, *148*, A1100–A1109.
(12) Sloop, S. E.; Pugh, J. K.; Wang, S.; Kerr, J. B.; Kinoshita, K. Chemical reactivity of PF_5 and $LiPF_6$ in ethylene carbonate/dimethyl carbonate. *Electrochem. Solid-State Lett.* **2001**, *4*, A42–A44.

(13) Kita, F.; Kawakami, A.; Nie, J.; Sonoda, T.; Kobayashi, H. On the characteristics of electrolytes with new lithium imide salts. *J. Power Sources* **1997**, *68*, 307–310.
(14) Barthel, J. M. G.; Krienke, H.; Kunz, W. *Physical Chemistry of Electrolyte Solutions: Modern Aspects*; Steinkopff Verlag: Darmstadt, Germany, 1998.
(15) Barthel, J.; Schmid, A.; Gores, H. J. A New Class of Electrochemically and Thermally Stable Lithium Salts for Lithium Battery Electrolytes. V. Synthesis and Properties of Lithium Bis[2,3-pyridinediolato(2−)-*O*,*O*′]borate. *J. Electrochem. Soc.* **2000**, *147*, 21–24.
(16) Schmidt, M.; Heider, U.; Kuehner, A.; Oesten, R.; Jungnitz, M.; Ignat'ev, N.; Sartori, P. Lithium fluoroalkylphosphates: a new class of conducting salts for electrolytes for high energy lithium-ion batteries. *J. Power Sources* **2001**, *97*−*98*, 557–560.
(17) Xu, W.; Shusterman, A. J.; Videa, M.; Velikov, V.; Marzke, R.; Angell, C. A. Structures of orthoborate anions and physical properties of their lithium salt nonaqueous solutions. *J. Electrochem. Soc.* **2003**, *150*, E74−E80.
(18) Krause, L. J.; Lamanna, W.; Summerfield, J.; Engle, M.; Korba, G.; Loch, R.; Atanasoski, R. Corrosion of aluminum at high voltages in non-aqueous electrolytes containing perfluoroalkylsulfonyl imides; new lithium salts for lithium-ion cells. *J. Power Sources* **1997**, *68*, 320–325.
(19) Xu, K. Nonaqueous liquid electrolytes for lithium-based rechargeable batteries. *Chem. Rev.* **2004**, *104*, 4303–4418.
(20) Zhang, X.; Devine, T. M. Passivation of aluminum in lithium-ion battery electrolytes with LiBOB. *J. Electrochem. Soc.* **2006**, *153*, B365–B369.
(21) Chen, Z.; Liu, J.; Amine, K. Lithium difluoro(oxalato)borate as salt for lithium-ion batteries. *Electrochem. Solid-State Lett.* **2007**, *10*, A45–A47.
(22) Zhang, S. S. Electrochemical study of the formation of a solid electrolyte interface on graphite in a $LiBC_2O_4F_2$-based electrolyte. *J. Power Sources* **2007**, *163*, 713–718.
(23) Zhang, S. S. An unique lithium salt for the improved electrolyte of Li-ion battery. *Electrochem. Commun.* **2006**, *8*, 1423–1428.
(24) Schreiner, C.; Amereller, M.; Gores, H. J. Chloride-Free Method To Synthesise New Ionic Liquids with Mixed Borate Anions. *Chem.*−*Eur. J.* **2009**, *15*, 2270–2272.
(25) Lee, H. S.; Yang, X. Q.; Sun, X.; McBreen, J. Synthesis of a new family of fluorinated boronate compounds as anion receptors and studies of their use as additives in lithium battery electrolytes. *J. Power Sources* **2001**, *97*−*98*, 566–569.
(26) Garcia, B.; Lavallée, S.; Perron, G.; Michot, C.; Armand, M. Room temperature molten salts as lithium battery electrolyte. *Electrochim. Acta* **2004**, *49*, 4583–4588.
(27) Abu-Lebdeh, Y.; Davidson, I. High-voltage electrolytes based on adiponitrile for Li-ion batteries. *J. Electrochem. Soc.* **2009**, *156*, A60–A65.
(28) Hagiwara, R.; Ito, Y. Room temperature ionic liquids of alkylimidazolium cations and fluoroanions. *J. Fluorine Chem.* **2000**, *105*, 221–227.
(29) Galinski, M.; Lewandowski, A.; Stepniak, I. Ionic liquids as electrolytes. *Electrochim. Acta* **2006**, *51*, 5567–5580.
(30) Carl, E. Neue Elektrolyte in organischen Carbonatloesungen zur Anwendung in sekundaeren Lithium-Ionen-Batterien. Ph.D. Thesis, University of Regensburg, Regensburg, Germany, 1998.
(31) Wachter, R.; Barthel, J. Untersuchungen zur Temperaturabhängigkeit der Eigenschaften von Elektrolytlösungen. *Ber. Bunsen-Ges. Phys. Chem.* **1979**, *83*, 634–642.
(32) Barthel, J. Electrolytes in non-aqueous solvents. *Pure Appl. Chem.* **1979**, *51*, 2093–2124.
(33) Casteel, J. F.; Amis, E. S. Specific conductance of concentrated solutions of magnesium salts in water−ethanol system. *J. Chem. Eng. Data* **1972**, *17*, 55–59.
(34) Schmidt, M.; Heider, U.; Kuehner, A.; Oesten, R.; Jungnitz, M.; Ignat'ev, N.; Sartori, P. Lithium fluoroalkylphosphates: a new class of conducting salts for electrolytes for high energy lithium-ion batteries. *J. Power Sources* **2001**, *97*−*98*, 557–560.
(35) Ding, M. S.; Jow, T. R. How Conductivities and Viscosities of PC−DEC and PC−EC Solutions of $LiBF_4$, $LiPF_6$, LiBOB, Et_4NBF_4, and Et_4NPF_6 Differ and Why. *J. Electrochem. Soc.* **2004**, *151*, A2007–A2015.
(36) Chu, A. C.; Josefowicz, J. Y.; Farrington, G. C. Electrochemistry of highly ordered pyrolytic graphite surface film formation observed by atomic force microscopy. *J. Electrochem. Soc.* **1997**, *144*, 4161–4169.
(37) Georen, P.; Lindbergh, G. On the use of voltammetric methods to determine electrochemical stability limits for lithium battery electrolytes. *J. Power Sources* **2003**, *124*, 213–220.
(38) Zhang, X.; Devine, T. M. Identity of Passive Film Formed on Aluminum in Li-Ion Battery Electrolytes with $LiPF_6$. *J. Electrochem. Soc.* **2006**, *153*, B344–B351.
(39) Zhang, X.; Devine, T. M. Factors That Influence Formation of AlF_3 Passive Film on Aluminum in Li-Ion Battery Electrolytes with $LiPF_6$. *J. Electrochem. Soc.* **2006**, *153*, B375–B383.
(40) Morita, M.; Shibata, T.; Yoshimoto, N.; Ishikawa, M. Anodic behavior of aluminum current collector in LiTFSI solutions with different solvent compositions. *J. Power Sources* **2003**, *119*−*121*, 784–788.

Received for review October 21, 2009. Accepted January 22, 2010. This work was supported by the Deutsche Forschungsgemeinschaft (DFG) in association with the "Projekt Initiative PAK 177, Funktionsmaterialien und Materialanalytik zu Lithium-Hochleistungsbatterien" (Contract 544243).

JE900867M